Microporous and Mesoporous Materials 148 (2012) 137–144

Contents lists available at SciVerse ScienceDirect

Microporous and Mesoporous Materials

journal homepage: www.elsevier.com/locate/micromeso

One-pot synthesis of silica monoliths with hierarchically porous structure

Glenna L. Drisko [a], Andrés Zelcer [b,c,*], Rachel A. Caruso [a,d,*], Galo J. de A.A. Soler-Illia [b,e]

[a] Particulate Fluids Processing Centre, School of Chemistry, The University of Melbourne, Melbourne, Victoria 3010, Australia
[b] Comisión Nacional de Energía Atomica, Gerencia Quimica, Avenida General Paz 1499, San Martin, Provincia de Buenos Aires 1650, Argentina
[c] Escuela de Ciencia y Tecnología, Universidad Nacional de San Martín, Argentina
[d] Commonwealth Scientific and Industrial Research Organization, Materials Science and Engineering, Clayton South, Victoria 3169, Australia
[e] Departamento de Química Inorgánica, Analítica y Química Física, Facultad de Ciencias Exactas y Naturales, Universidad de Buenos Aires, Argentina

ARTICLE INFO

Article history:
Received 7 June 2011
Received in revised form 1 August 2011
Accepted 2 August 2011
Available online 7 August 2011

Keywords:
Polymerization-induced phase separation
Monolith
Hierarchical pore structures
Silica
Furfuryl alcohol

ABSTRACT

Poly(furfuryl alcohol) (PFA) and block copolymer Pluronic F127 were used as pore templates to create mechanically robust silica monoliths with a hierarchical and interconnected macro–mesoporous network in an easy, reproducible bimodal scale templating process. Control over the morphology was obtained by varying the reactant ratios. Phase separation on the submicrometer scale occurred when furfuryl alcohol was cationically polymerized and therefore became immiscible with the solvent and the silica precursor. Upon a subsequent sol–gel reaction, a silica-F127 matrix formed around the PFA spheres, leading to macropore structures with mesoporous walls. Surface areas of the final structures ranged from 500 to 989 $m^2 g^{-1}$ and a maximum pore volume of 4.5 mL g^{-1} was achieved. Under mildly acidic conditions, micelle-templated mesopores resulted. Interconnected macropores could be obtained by increasing the pH or the block copolymer concentration. The formation mechanism and the relationship between PFA, Pluronic F127 and acidity are discussed in detail.

1. Introduction

Simple and inexpensive procedures are needed to produce multi-scale structured silica monoliths [1]. Diverse morphologies are required due to the wide variety of applications for these materials, such as sorption/separation, biomaterials engineering, membrane-based reactors and scaffolds for the formation of hierarchical carbon materials [2–4]. Hierarchical pore structures are ideal for applications where a solid material is in contact with a fluid phase because the macropores allow the fluid to quickly reach the high internal surface area provided by meso- or micropores [5]. Hierarchical structures are especially useful in the case of macroscopic materials, in which fast transport of molecules (solvent, reactants, products, probes, analytes, etc.) throughout the whole material is critical, as diffusion pathways are comparatively long [6,7]. The size and structure of the macropores effects diffusion rate and capacity; therefore material architecture must be constructed to meet the needs of each application [8,9]. The human body gives two excellent examples of how effectively hierarchical systems work: the respiratory system [10], and the circulatory system, where the presence of increasingly smaller features maximizes flow and exchange rates. By following nature's example, effective designs can be created for a host of structured materials.

Monoliths are more practical than thin films or compacted powders for many applications, due to their robustness and ease of handling. The hierarchical pore architecture is especially important in macroscopic materials, as macroporosity is needed to encourage rapid access to internal porosity [7–9]. In the traditional templating approach, monoliths, thick films or xerogels with hierarchical porosity are prepared by using colloidal particles or pre-organized structures as sacrificial scaffolds [6,11–16]. While these techniques are capable of producing very complex structures of highly controllable dimensions, it often requires separate steps for the template preparation and the structure transfer. In order for hierarchically porous monoliths to be produced on an industrial scale, they must be prepared using cheap starting materials and through a simple method that is relatively insensitive to the changes in ambient conditions.

An alternative to templating preformed structures is to use emulsions or foams to produce porous silica. While this approach permits the continuous preparation of material, particular attention must be paid to the synthesis conditions, for the precursor systems are very sensitive to small variations in the composition [17,18]. Another option is to use glycol modified silanes as precursors to construct hybrid materials with well-defined hierarchical porosity [19].

* Corresponding authors at: Comisión Nacional de Energía Atomica, Gerencia Quimica, Avenida General Paz 1499, San Martin, Provincia de Buenos Aires 1650, Argentina. Tel.: +54 11 6772 7032; fax: +54 11 6772 7886 (A. Zelcer), Particulate Fluids Processing Centre, School of Chemistry, The University of Melbourne, Melbourne, Victoria 3010, Australia. Tel.: +61 3 8344 7146; fax: +61 3 9347 5180 (R.A. Caruso).

E-mail addresses: zelcer@cnea.gov.ar (A. Zelcer), rcaruso@unimelb.edu.au (R.A. Caruso).

1387-1811/$ - see front matter © 2011 Elsevier Inc. All rights reserved.
doi:10.1016/j.micromeso.2011.08.007

Phase separation is an attractive technique for synthesizing multiscale structured materials inexpensively and reproducibly. However, the instigative force of phase separation is crucial and must be thoroughly studied to achieve tailorability of the morphology. Nakanishi has pioneered phase separation through spinodal decomposition of polymers in solution as a means to produce macroporous inorganic monoliths in a single-step reaction, followed by calcination [20]. Generally, a silica precursor, the structure directing agent(s) (polymers or polymeric surfactants) and a solvent are mixed together and after inorganic condensation, evaporation and calcination, macroporous oxide results. The macropore size and pore volume can be controlled independently by varying the quantities of polymer and solvent [20]. Due to the strength of the driving forces involved, the morphologies created by spinodal decomposition change greatly with small variations of reagent ratios [21], curing temperature or other conditions. Obtaining a homogeneous structural evolution of the phase separation relative to the inorganic gelation requires precise selection of reagents, molar ratios and processing temperature [22].

An alternative to spinodal decomposition is to use polymerization-induced phase separation to produce the macroporous structure. We have recently reported a general method for the production of macroporous–mesoporous oxides, in which multiscale templating can be achieved in a one-pot synthesis using furfuryl alcohol (FA), Pluronic F127 and an oxide precursor [23]. The versatility of this method arises from the *in situ* formation of a macropore template of varying hydrophobicity, morphology and dimensions. PFA can be generated from inexpensive FA via a cationic polymerization (Scheme 1), initiated by protic acids [24] or Lewis acids, such as titanium, tin and zinc cations [25,26]. As PFA grows in molecular weight and forms crosslinks, it becomes more hydrophobic and phase separates from the reaction mixture [27]. The resulting polymerization-induced phase separation has been used to create composites of silica and carbon [28,29]. Porous carbon materials were produced by treating the composite with hydrofluoric acid to dissolve the silica. Previous reports of inorganic monoliths prepared from tetraethyl orthosilicate (TEOS), FA and acid [30], did not make use of a block copolymer to control the formation of mesopores. High temperatures (900 °C) were needed to remove the carbonaceous template, yielding materials with relatively modest surface areas (200 $m^2 g^{-1}$) and disconnected macropores.

In the present report we describe the combination of two templates, PFA and Pluronic F127, to form hierarchically porous silica monoliths using polymerization-induced phase separation. The macropore architecture is adjustable and can be interconnected. Surfactant-templated mesoporosity results in nearly five times higher surface areas than previously reported PFA-templated silica monoliths [30]. A range of preparation conditions was explored to elucidate the formation mechanism of hierarchically porous silica monoliths, and to achieve control in the pore structure and size. Our results show that pH plays a critical role in the interaction between the mesoporogen (Pluronic F127) and macroporogen (PFA), and in the condensation kinetics of PFA and the silica matrix. These thermodynamic and kinetic aspects are essential to understand the co-assembly of the different building blocks (silica and FA oligomers, F127 micelles or other aggregates). When these interactions are understood, the properties of the material, *e.g.* pore size, morphology and surface area, can be controlled. This work is an important step towards the ultimate goal: silica with tailored porosity across multiple scales.

2. Experimental section

2.1. Materials

Ethanol was purchased from Merck. FA, TEOS and Pluronic F127 were obtained from Sigma Aldrich, while 37% hydrochloric acid (HCl) was purchased from Scharlau. To obtain a hydrophilic silica precursor, a prehydrolyzed solution was prepared in the following way: TEOS (20.8 g), ethanol (13.8 g) and 1.8 g of 0.14 M HCl were combined and refluxed for 2 h. The solution was allowed to cool and was then stored at 4 °C in an airtight container. The 0.14 M HCl solution was produced by combining 2.3 mL of 37% HCl with 198 mL of MilliQ water. The 5.00 M HCl solution was prepared by combining 1 mL 37% HCl and 1.4 mL of MilliQ water, whereas 0.12 M HCl was a combination of 1 mL 37% HCl and 99 mL of MilliQ water.

2.2. Synthesis of silica monoliths [23]

Pluronic F127 (F127, 0–0.258 g) was weighed into vials and dissolved in 0.12 M or 5.00 M hydrochloric acid (0.33 g) and hydrolyzed silica precursor (0.50 g, 1.394 mmol). FA (0–1.36 g) was added to the solutions, and after mixing well for ~2 min, the caps were removed from the vial and the solvent was allowed to evaporate slowly under ambient conditions. Samples were moved to a 65 °C oven for 3 days, followed by 2 days in a 135 °C oven. The samples were calcined under a low air flow using the following program: 10 °C min^{-1} 20–130 °C, 2 °C min^{-1} to 450 °C, 1 °C min^{-1} to 550 °C, the maximum temperature at which samples were calcined for 2 h. The quantities added to achieve specific molar ratios are listed in Table 1.

2.3. Characterization and equipment

Mercury intrusion porosimetry was used to measure the volume and size distribution of the macropores. Samples were

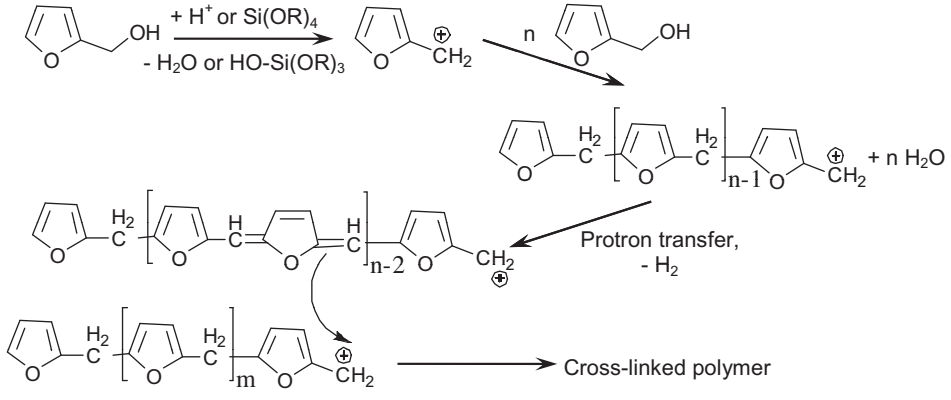

Scheme 1. Example structure of PFA formed by cationic polymerization, where *n* and *m* represent the number of monomer units [30].

Table 1
The amount of F127, FA and HCl used to obtain the desired molar equivalents, in relation to 1 Si.

Reagent	Quantity added (g)	Quantity added (mmol)	Molar equivalents to Si
F127	0.017	0.00000135	0.0010
	0.043	0.0000341	0.0025
	0.086	0.00000683	0.0049
	0.129	0.0000102	0.0073
	0.172	0.0000137	0.0098
	0.258	0.0000205	0.0147
Furfuryl alcohol	0.14	1.43	1.03
	0.34	3.47	2.49
	0.68	6.93	4.99
	1.02	10.4	7.48
	1.36	13.9	9.97
0.12 M HCl	0.33	0.037	0.027
5.00 M HCl	0.33	1.525	1.10

degassed at 150 °C before measurement using a Micromeritics VacPrep 061 attached to a heating station. A 14-0411 penetrometer with a 3 mL bulb was loaded with the sample. The measurement was conducted on a Micromeritics AutoPore III with pressure ranging from 13.8 to 413,700 kPa. The data was collected and analyzed using Win9420 V1.01.

The surface area and mesopore sizes of the synthesized materials were measured using nitrogen physisorption on a Micromeritics TriStar 3000 instrument. Samples were degassed at 150 °C and at a pressure of approximately 6.6 kPa for a minimum of 4 h prior to analysis using a Micromeritics VacPrep 061. The surface area was calculated using the Brunauer–Emmett–Teller (BET) method. Barrett–Joyner–Halenda (BJH) was used to calculate the mesopore size distribution using the adsorption branch.

Scanning electron microscopy (SEM) was performed on a FEI QUANTA 200F microscope operated at voltages between 15 and 20 kV. Samples were mounted on carbon coated SEM stubs and then sputter coated with a thin layer of gold using an Edwards S150B Gold Sputter Coater.

Small angle X-ray scattering (SAXS) data was obtained on the SAXS2 line of the Laboratorio Nacional de Luz Sincrotron (Brazil), using 8 keV radiation and a bidimensional detector. Samples were ground and placed between two kapton sheets. The configuration allowed for the analysis of q spacings ranging from 0.19 to 4 nm^{-1}.

Transmission electron microscopy (TEM) analyses were conducted using a Philips CM120 BioTWIN microscope operating at 120 kV. TEM samples were prepared by finely grinding the sample in ethanol using an agate mortar and pestle, sonicating for 20 min and then drop depositing the solution on to carbon-coated copper grids.

3. Results

3.1. The synthesis of SiO_2 monoliths

Using the PFA-F127 templating method reported here, we obtained intact porous SiO_2 monoliths after gelation-drying. After a mild thermal treatment, a SiO_2-PFA composite is obtained (Fig. 1a). PFA is compliant to the shrinkage produced upon SiO_2 condensation: during the thermal treatment the excess PFA exudes from the monoliths, producing a black cracked shell around the monolith. Fig. 1b shows a photograph of a calcined sample held between fingers. During the gelation-drying stage, a phase separation took place, generating organic-rich and inorganic-rich phases [30]. The separation of PFA from water, ethanol and the inorganic precursor led to the formation of micrometer-sized spherical polymeric particles [23]. Upon solvent and acid evaporation, the pH increased, triggering silica gelation around the polymer droplets and yielding a composite of PFA embedded in a SiO_2 matrix (Fig. 1c). The material hardened taking the form of the vial mold. Calcination of the hybrid PFA-F127-silica monolith eliminated the organic matter, forming macrocavities in the space where the PFA spheres had resided (Fig. 1d). Performing the polymerization *in situ* circumvented the need for separate colloidal template preparation and purification steps. Moreover, a one-pot synthesis avoids a re-dispersion step [31] or the need for colloidal surface modification [32], which are problems often associated with the use of colloidal templates.

3.2. The role of FA

Furfuryl alcohol was necessary to induce macroporosity in the monolithic silica. Upon addition of acid, furfuryl alcohol polymerized, cross-linked and thereby became hydrophobic; separating from the aqueous solution in a polymerization-induced phase separation. When no FA was added to the initial mixtures, macropores were absent (Fig. 2a). As the [FA]/[Si] molar ratio was increased, the macroporosity began to increase (Fig. 2b), eventually becoming an interconnected network (see [FA]/[Si] = 10, Fig. 2c). The volume of macroporosity (measured by mercury intrusion porosimetry) was shown to increase when higher quantities of FA were used in the synthesis (Fig. 2d), for instance, the total pore volumes of the materials shown in Fig. 2a–c were 0.42, 2.6 and 4.5 mL g^{-1}, respectively.

3.3. The role of Pluronic F127

The hierarchically porous silica monoliths demonstrated Type IV sorption isotherms when analysed by nitrogen sorption (Fig. 3a). H1 hysteresis loops were observed when the sample was prepared in the absence of block copolymer, which is typically ascribed to agglomerates of particles. On the other hand, samples produced with 0.005–0.010 mol F127 to Si demonstrated H2 hysteresis character with loop closure at 0.60–0.65 P/P^0. For samples prepared using F127, the mesopore volume increased with increasing concentration of F127 in the synthesis solution (Fig. 3b). As expected for an evaporation-induced self-assembly (EISA) mechanism, the average size of the mesopores did not vary significantly with increases in the F127 concentration, as has been seen in titania/PFA/F127 systems [23], yet the distribution did narrow. In the absence of surfactant, the mesopores were much smaller in volume and diameter (i.e., 3.5 vs. ca. 10 nm, see Fig. 3b), as derived from the nitrogen adsorption data. All samples demonstrated significant amounts of microporosity, due to incomplete condensation between neighboring silica chains. No mesopores were detected by gas sorption in non-calcined samples (data not shown), indicating that the initially obtained hybrid materials were filled with organic matter [30,33]; that is F127 and PFA.

As the molar ratio of [F127]/[Si] increased from 0 to 0.0100, the pore volume (BJH, measured with nitrogen adsorption) increased from 1.0 to 1.8 $cm^3\ g^{-1}$ (Fig. 4). This coincided with a decrease in BET surface area, from 989 $m^2\ g^{-1}$ when [F127]/[Si] = 0 was used to 788 $m^2\ g^{-1}$ when [F127]/[Si] = 0.0100.

When $[H^+]$ was high, the amount of F127 used during synthesis affected the size and connectivity of the micrometer sized PFA spheres and thus the macropore architecture, as shown in Fig. 5. If no F127 was added to the solution, the spheres were disconnected. As the [F127]/[Si] mole ratio increased, the void space increased. When [F127]/[Si] reached 0.015, a less regular and interconnected structure was produced (Fig. 5c). These effects might be ascribed to the interactions of the block copolymer with the PFA particles, which would be more marked at higher block copolymer concentration. With little or no F127 present, the high tension of the aqueous-PFA interface led to minimization of the

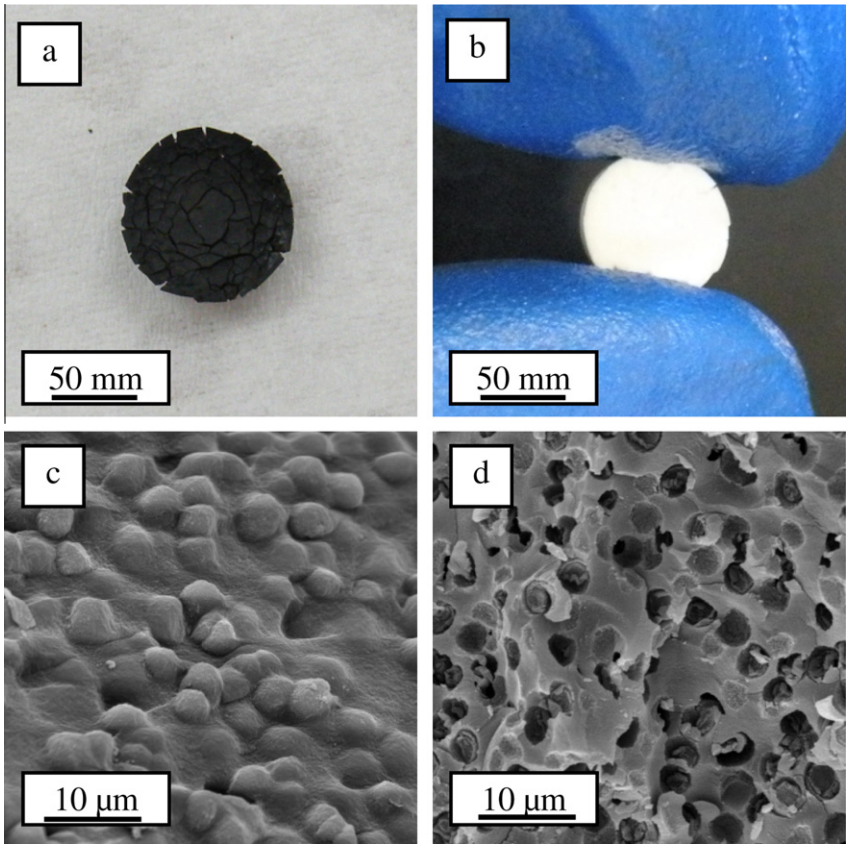

Fig. 1. Photograph of a typical silica monolith prepared using PFA and F127 templates (a) before calcination and (b) after calcination at 550 °C. SEM images (c) before and (d) after calcination at 550 °C.

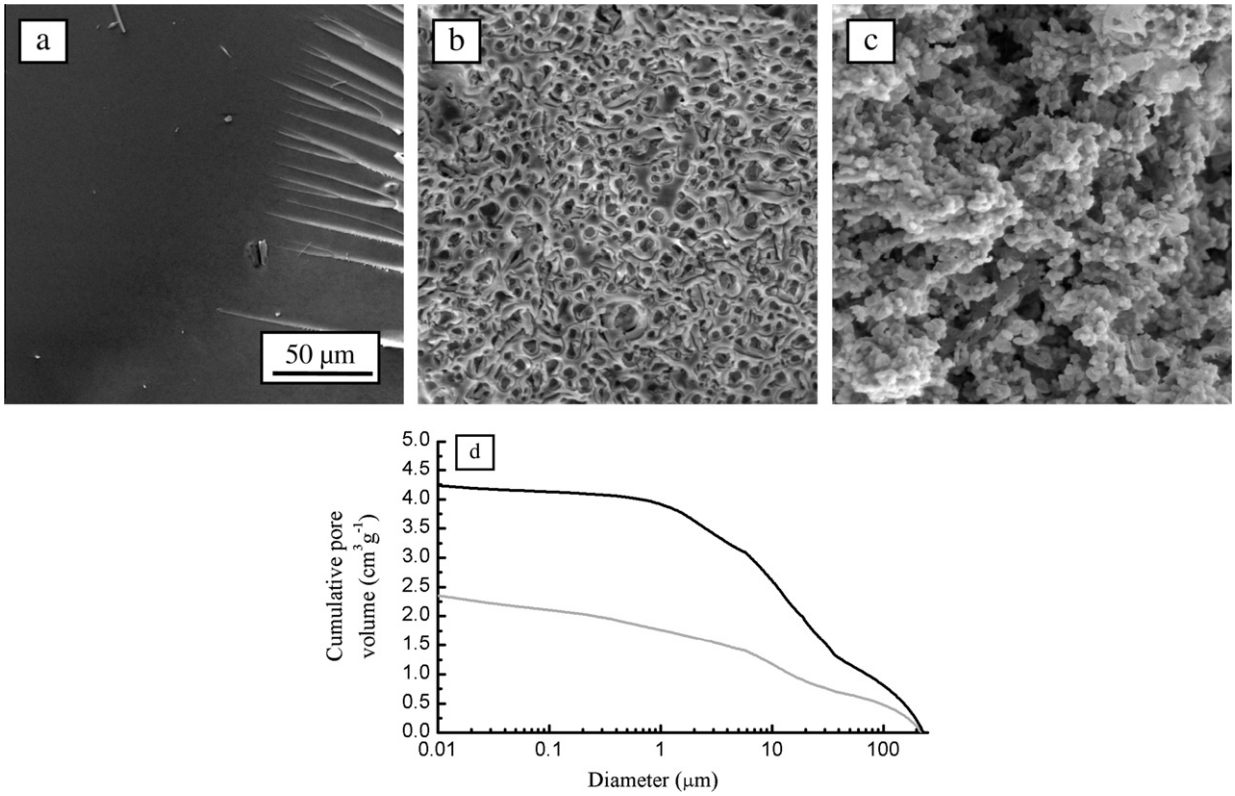

Fig. 2. SEM images of the samples produced using the following [FA]/[Si]: (a) 0, (b) 2.5 and (c) 10. (d) Mercury intrusion porosimetry plots of monoliths produced with 7.5 (grey line) and 10 M equivalents of FA (black line). Samples were synthesized using 1 Si:0.005 F127:*x* FA:1.10 HCl. The scale is the same for all SEM images.

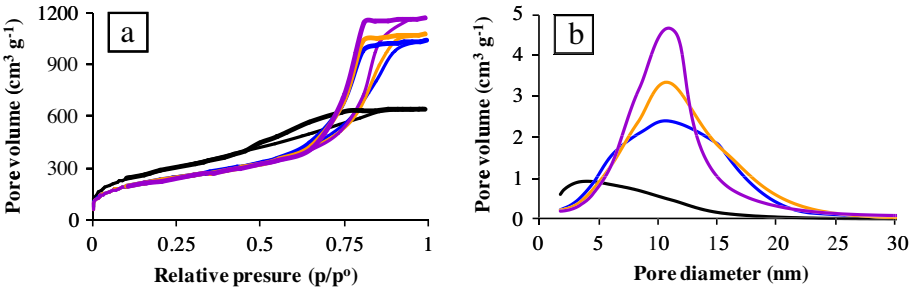

Fig. 3. (a) Nitrogen sorption isotherms and (b) BJH pore size distributions of samples produced with increasing quantities of [F127]/[Si]: 0.000 (black), 0.0050 (blue), 0.0075 (orange) and 0.0100 (purple). The synthesis mixture contained 1 Si:*x* F127:5 FA:0.03 HCl. (For interpretation of the references to color in this figure legend, the reader is referred to the web version of this article.)

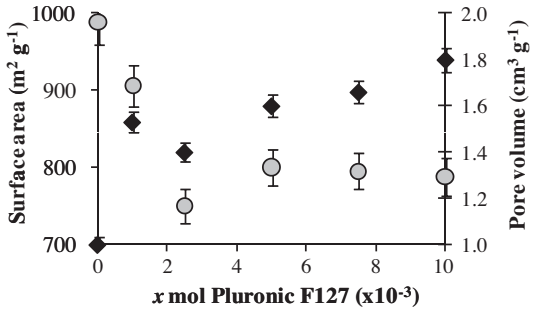

Fig. 4. Surface area (grey circles) and BET pore volume (black diamonds) of silica monoliths made with molar ratios of 1 Si:*x* Pluronic F127:5 FA:0.03 HCl.

PFA surface area, and thus the PFA existed as discrete spheres (Fig. 5a and b). Upon increasing surfactant concentration, the surface tension lowered and the interfaces became more diffuse (Fig. 5c), rendering less regular-shaped and more interconnected macropores, presenting good accessibility through the whole monolith.

3.4. The role of acid concentration

When the mole ratio of acid to silicon, was kept relatively low during the synthesis ($[H^+]/[Si] = 0.03$), micelle-templated mesopores of the calcined material were observable in the TEM (Fig. 6a). SAXS analysis of the calcined sample displayed a strong scattering peak corresponding to a characteristic distance of 10.2 nm (Fig. 6b). Only one reflection is observed, indicating short-range order within the structure. Under more acidic synthesis conditions using $[H^+]/[Si] = 1.10$, TEM images display a different aspect: denser silica walls appear as nanoparticle arrays loosely organized around smaller, more polydisperse mesopores, as shown in Fig. 6c. Only a diffuse scattering background is observed in SAXS. In this case, the mesoporosity of the final materials seemed to be due to interparticle cavities, i.e., the origin of mesopores is textural, rather than templated.

4. Discussion

Under the synthesis conditions explored in this study, the addition of F127 was crucial to the stability of the silica monoliths. Calcination of materials produced with the block copolymer resulted in intact monoliths, which could be handled with tweezers or fingers (Fig. 1b). However, in the absence of F127, the materials collapsed upon template removal. F127 has indeed an effect on the pore structure: templated samples present a more regular pore size and interconnectivity, as well as thicker walls that likely indicate a more extensive silica condensation. This last factor is known to improve the mechanical properties of mesoporous silica [34]. The materials produced previously using only PFA as the sole template were sintered at high temperature (900 °C) to obtain a robust material, yielding a relatively low surface area of 213 $m^2 g^{-1}$ [30]. This need for high sintering temperatures might be due to poor pore interconnectivity, which hinders total pyrolysis of the carbon component. In this study, lower calcination temperatures were possible, leading to substantially higher surface areas (up to 989 $m^2 g^{-1}$). Moreover, lower calcination temperatures require less energy, and thus decrease the processing costs of the final product.

The nature of the interactions between PFA, F127 and the SiO_2 oligomers was pH dependent. Changing concentration of the macroporogen had little effect on the mesopore structure at high acid

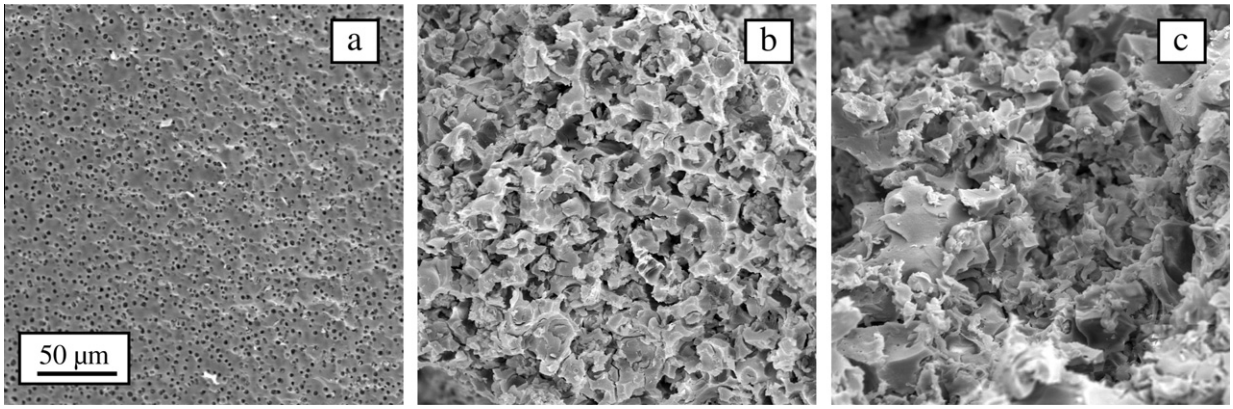

Fig. 5. SEM micrographs of samples prepared with [F127]/[Si] = (a) 0.0000, (b) 0.0050 and (c) 0.0100. The samples were prepared with a molar ratio of 1 Si:*x* F127:5 FA:1.10 HCl. The scale is the same for all images.

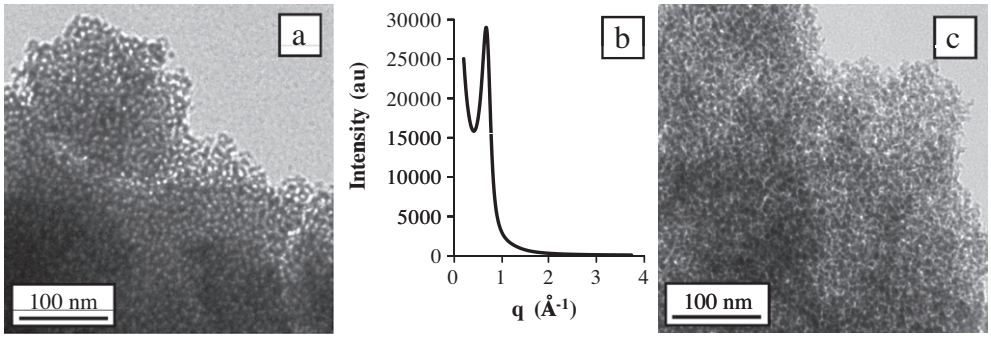

Fig. 6. (a) TEM image and (b) SAXS pattern of a silica monolith produced from $[H^+]/[Si] = 0.03$. (c) TEM image of a monolith produced from $[H^+]/[Si] = 1.10$. A solution of 1 Si: 0.0075 F127:1 FA:*x* HCl was used.

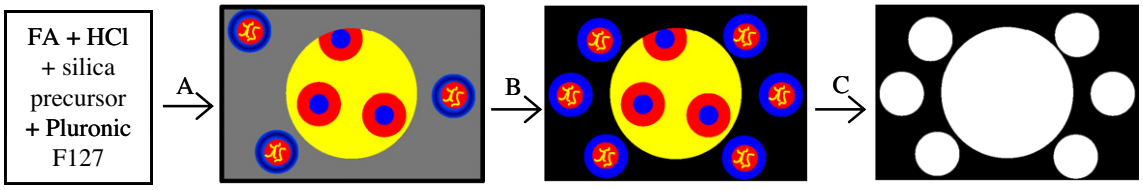

Fig. 7. When $[H^+]/[Si] = 0.03$, the synthesis proceeds in three steps: (A) Polymerization of FA (yellow) and phase separation from the sol (grey). F127 forms micelles (blue PEO shell, red PPO core) with the PPO domain enlarged with FA oligomers (yellow). PFA spheres also contain F127 inverse micelles (red PPO shell, blue PEO core). (B) Gelation of the silica phase (black) around the PFA (yellow) and the F127 (PEO block blue, PPO block red). (C) Calcination of the hybrid material at 550 °C produced well-defined meso- and macropores (white) within the silica matrix. Not drawn to scale. (For interpretation of the references to colour in this figure legend, the reader is referred to the web version of this article.)

concentrations, but did have an effect under more mild acidity. Moreover, pH has a large effect over the sol–gel behavior of silica. Thus the following discussion of the mechanism is divided into two parts, low and high H^+ concentration, each part discussing the three important concurrent processes: (a) FA polymerization behavior, (b) F127 assembly behavior and (c) SiO_2 condensation rate.

The scheme in Fig. 7 summarizes the model proposed for relatively mildly acidic conditions, i.e., $[HCl]/[Si] = 0.03$. The polymerization of FA is slower and crosslinking occurs to a lesser degree by the time SiO_2 gelation takes place. Therefore, PFA particles are less hydrophobic, less rigid and organic oligomers persist in solution. The PFA particles are compatible with the polypropylene oxide (PPO) block of F127, therefore PFA can be swollen with inverse micelles of the surfactant [35]. Spherical macropores for all F127:FA ratios studied could be observed.

Under these conditions, small FA oligomers may enter the PPO block of the F127 micelles in the solution (Fig. 7), which can increase the width of the mesopore size distribution and volume (Supplementary Fig. S1a). This is similar to polypropylene glycol, which has been reported to swell F127 micelles [36]. The mild conditions permitted the assembly of block copolymer micelles with short range order (Fig. 6a and b).

When $[H^+]/[Si] = 0.03$ in the initial stage of synthesis, the silica condensation rate was near a minimum (pH values between 1 and 3) [37], giving rise to low molecular weight mostly linear inorganic polymers. Therefore individual silica particles were not observed when $[H^+]/[Si] = 0.03$ was used (Fig. 6a). The inorganic condensation rate increases upon evaporation of the solvent and acid; gentle silica gelation around the surfactant assembly leads to a consolidated mesostructured material in a classical EISA pathway [38,39].

In contrast, under strongly acidic conditions ($[H^+]/[Si] = 1.10$, proposed synthesis scheme shown in Fig. 8), the degree of polymerization and crosslinking of FA and silica were significantly higher [25]. The higher molecular weight, more hydrophobic FA polymers increase the degree of phase separation, leading to interconnected macropores for higher FA concentration (Fig. 2c). Lower pH also resulted in decreased compatibility between F127 and PFA, as compared to previous work, [40] and that which we report for $[HCl]/[Si] = 0.03$. The highly crosslinked PFA particles were less able to swell, therefore F127 resided in the sol.

In the early stages of reaction, Pluronic F127 did not form micelles because the concentration was below the critical micelle concentration (cmc), which lies between 0.397 and 0.431 mM at 25 °C [41,42]. In the solution with the highest F127 content, 1

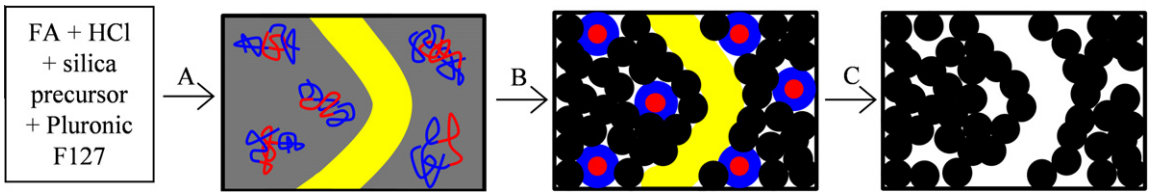

Fig. 8. Under harsher acidity, $[HCl]/[Si] = 1.10$, the synthesis proceeds in three steps: (A) Polymerization of FA (yellow) and phase separation from the sol (grey). The PFA phase separates and the non-assembled F127 (blue and red) stabilizes the silica sol. (B) Gelation of the silica phase (black) around the PFA (yellow) and the F127 (PEO block blue, PPO block red). Upon solvent evaporation, the F127 forms micelles, but the silica particles are too large to template the assembled structure. (C) Calcination of the hybrid material at 550 °C produces textural porosity and macrovoids (white) within the silica matrix. Not drawn to scale. (For interpretation of the references to colour in this figure legend, the reader is referred to the web version of this article.)

Si:0.015 Pluronic F127:5 FA:1.10 HCl, the initial F127 concentration is 0.0137 mM, an order of magnitude lower than the cmc. The acid concentration does not need to be considered for Pluronic F127 micelle formation [43], although as pH is lowered from pH 7.4 to 2, the polyethylene oxide (PEO) block does become more hydrophilic due to its high polarizability [44]. The late onset of micelle formation (requiring solvent evaporation) proved to be detrimental to effective templating, as will be explained below. Therefore, at [HCl]/[Si] = 1.10, varying FA concentration had little effect on silica mesopore size (3–5 nm), volume (0.42–0.59 g cm^{-3}) and surface area (544–705 m^2 g^{-1}) (Supplementary see Figs. S1b and S2).

The condensation rate of the silica precursor is faster at high initial acidity (pH < 1) [37]. The net effect of the higher inorganic reactivity is that Si-oxo oligomers form in the early stages of the reaction, probably stabilized by interactions with the block copolymer. With solvent evaporation the F127 would begin to form micelles. However, the inorganic clusters that had grown earlier were too large to co-assemble around the F127 micelles. The size mismatch resulted in a disordered textural mesoporosity [45,46]. Only a minimal degree of particle growth is likely to have occurred during the prehydrolysis of TEOS, as has been observed in other studies [47].

Thus, changing from low to high acidities affected thermodynamic factors such as the degree of polymerization (i.e., size of the silica and PFA building blocks) and the interplay between PFA, F127 and silica, as well as the polymerization kinetics of both silica and PFA. Control of these aspects is essential to understanding the formation processes of the macro- and the mesopores, which permits tuning of the hierarchical pore architecture.

5. Conclusions

Monoliths with hierarchical macro–mesoporous structure were produced in the shape of the mold through a combination of block copolymer and PFA templating. Mechanically stable systems with high surface areas and well-defined tuneable pore size over two length scales have been produced. Interconnected macropores could be obtained by using highly acidic synthesis solutions with a minimum of 5 M equivalents of FA to Si, or by increasing the concentration of Pluronic F127. However, the high proton concentration led to large silica particle growth before the cmc of F127 was reached. The assembly of silica around the block copolymer micelles was disrupted and therefore small diameter (~5 nm) mesopores, with a rather large size distribution derived from interparticle voids, were obtained. Under less acidic synthesis conditions, PFA and silica condensation were slower and thus micelle-templated mesopores of 10 nm diameter mesopores with local order were produced, which permitted the preparation of intact macroporous–mesoporous monoliths at relatively low calcination temperatures. Our findings indicate that the templates do not act independently, especially when [HCl]/[Si] = 0.03, rather an interaction between the two porogens occurs, allowing the pore architecture to be tuned through the control of co-assembly and polymerization kinetics.

The FA concentration was a strong determinant of PFA particle size. Macropores were not present when FA was absent from the reaction mixture, while very well connected macropores were observed when $\geqslant$7.5 M equivalents FA to Si were used in combination with high concentrations of acid. This method does not require a precise synchronization between the gelation of the inorganic and phase separation of the organic template, and therefore is a robust method that functions over a wide variety of Si:template ratios. Our findings suggest that further decoupling of SiO_2 hydrolysis-condensation and FA polymerization could lead to greater control of pore sizes and volumes. Additionally we will be pursuing materials that contain both ordered mesoporosity and interconnected macropores using low acidity conditions.

Acknowledgements

Prof. Yi-Bing Cheng and his high temperature ceramics subgroup, particularly Dr. Kun Wang, are thanked for enlightening discussions about this research. Financial support for travel by GLD from The University of Melbourne to Comisión Nacional de Energía Atómica was generously provided by The University of Melbourne Postgraduate Overseas Research Experience Scholarships (PORES) and an Australian Research Council Nanotechnology Network Overseas Travel Fellowship. GLD was supported by the Albert Shimmins Memorial Fund while writing this manuscript. The synchrotron experiments were conducted at the Laboratorio Nacional de Luz Sincrotron (LNLS) in Campinas, Brazil under scientific project 5353. This research was financially supported by a Discovery Project from the Australian Research Council (DP0877428) and Argentina's Agencia Nacional de Promocion Científica y Tecnológica (ANPCyT PICT 34518, PICT 1848, PAE 2004 22711, PAE-PME 2007-00038). AZ acknowledges Conicet for his postdoctoral fellowship. GJAASI and AZ are Conicet researchers. RAC acknowledges the Australian Research Council for a Future Fellowship (FT0990583).

Appendix A. Supplementary data

Supplementary data associated with this article can be found, in the online version, at doi:10.1016/j.micromeso.2011.08.007.

References

[1] B.-L. Su, A. Vantomme, L. Surahy, R. Pirard, J.-P. Pirard, Chem. Mater. 19 (2007) 3325–3333.
[2] Z.-Y. Yuan, B.-L. Su, J. Mater. Chem. 16 (2006) 663–677.
[3] R. Backov, Soft Matter 2 (2006) 452–464.
[4] E. Prouzet, S. Ravaine, C. Sanchez, R. Backov, New J. Chem. 32 (2008) 1284–1299.
[5] P. Innocenzi, L. Malfatti, G.J.A.A. Soler-Illia, Chem. Mater. 23 (2011) 2501–2509.
[6] P. Colombo, C. Vakifahmetoglu, S. Costacurta, J. Mater. Sci. 45 (2010) 5425–5455.
[7] G.L. Drisko, V. Luca, E. Sizgek, N. Scales, R.A. Caruso, Langmuir 25 (2009) 5286–5293.
[8] G.L. Drisko, M. Chee Kimling, N. Scales, A. Ide, E. Sizgek, R.A. Caruso, V. Luca, Langmuir 26 (2010) 17581–17588.
[9] G.L. Drisko, P. Imperia, M. Reyes, V. Luca, R.A. Caruso, Langmuir 26 (2010) 14203–14209.
[10] M.S. Gordon, Animal Physiology: Principles and Adaptations, Macmillan, New York, 1979.
[11] G.L. Drisko, X. Wang, R.A. Caruso, Langmuir 27 (2011) 2124–2127.
[12] L.-L. Li, W.-T. Duan, Q. Yuan, Z.-X. Li, H.-H. Duan, C.-H. Yan, Chem. Commun. (2009) 6174–6176.
[13] A.-H. Lu, F. Schüth, Adv. Mater. 18 (2006) 1793–1805.
[14] A. Stein, F. Li, N.R. Denny, Chem. Mater. 20 (2008) 649–666.
[15] C.M. Doherty, R.A. Caruso, B.M. Smarsly, P. Adelhelm, C.J. Drummond, Chem. Mater. 21 (2009) 5300–5306.
[16] S. Sotiropoulou, Y. Sierra-Sastre, S.S. Mark, C.A. Batt, Chem. Mater. 20 (2008) 821–834.
[17] N. Brun, S. Ungureanu, H. Deleuze, R. Backov, Chem. Soc. Rev. 40 (2011) 771–788.
[18] P. Schmidt-Winkel, C.J. Glinka, G.D. Stucky, Langmuir 16 (2000) 356–361.
[19] S. Hartmann, D. Brandhuber, N. Hüsing, Acc. Chem. Res. 40 (2007) 885–894.
[20] K. Nakanishi, N. Tanaka, Acc. Chem. Rev. 40 (2007) 863–873.
[21] J. Konishi, K. Fujita, K. Nakanishi, K. Hirao, Chem. Mater. 18 (2006) 6069–6074.
[22] J. Konishi, K. Fujita, S. Oiwa, K. Nakanishi, K. Hirao, Chem. Mater. 20 (2008) 2165–2173.
[23] G.L. Drisko, A. Zelcer, V. Luca, R.A. Caruso, G.J.A.A. Soler-Illia, Chem. Mater. 22 (2010) 4379–4385.
[24] S. Bertarione, F. Bonino, F. Cesano, A. Damin, D. Scarano, A. Zecchina, J. Phys. Chem. B 112 (2008) 2580–2589.
[25] M. Choura, N.M. Belgacem, A. Gandini, Macromolecules 29 (1996) 3839–3850.
[26] F. Cesano, D. Scarano, S. Bertarione, F. Bonino, A. Damin, S. Bordiga, C. Prestipino, C. Lamberti, A. Zecchina, J. Photochem. Photobiol. A 196 (2008) 143–153.
[27] A. Gandini, M.N. Belgacem, Prog. Polym. Sci. 22 (1997) 1203–1379.

[28] D. Kawashima, T. Aihara, Y. Kobayashi, T. Kyotani, A. Tomita, Chem. Mater. 12 (2000) 3397–3401.
[29] H. Müller, P. Rehak, C. Jäger, J. Hartmann, N. Meyer, S. Spange, Adv. Mater. 12 (2000) 1671–1675.
[30] S. Grund, A. Seifert, G. Baumann, W. Baumann, G. Marx, M. Kehr, S. Spange, Microporous Mesoporous Mater. 95 (2006) 206–212.
[31] D. Myers, Surfaces, Interfaces and Colloids: Principles and Applications, second ed., Wiley-VCH, New York, 1999.
[32] M. Antonietti, B. Berton, C. Göltner, H.-P. Hentze, Adv. Mater. 10 (1998) 154–159.
[33] D. Chen, L. Cao, F. Huang, Y.B. Cheng, R.A. Caruso, J. Am. Chem. Soc. 132 (2010) 4438–4444.
[34] F. Ciaramella, V. Jousseaume, S. Maitrejean, M. Verdier, B. Remiat, A. Zenasni, G. Passemard, Thin Solid Films 495 (2006) 124–129.
[35] K. Wang, Controlling Nanostructures of Si-based Ceramics via Carbothermal Reduction of Mesoporous Silica-Carbon Nanocomposites, Ph.D. Thesis, Monash University, Melbourne, 2010.
[36] L. Malfatti, M.G. Bellino, P. Innocenzi, G.J.A.A. Soler-Illia, Chem. Mater. 21 (2009) 2763–2769.
[37] C.J. Brinker, G.W. Scherer, Sol-Gel Science: The Physics and Chemistry of Sol-Gel processing, Academic Press Inc., San Diego, 1990 (Chapter 3).
[38] D. Grosso, F. Cagnol, G.J.A.A. Soler-Illia, E.L. Crepaldi, H. Amenitsch, A. Brunet-Bruneau, A. Bourgeois, C. Sanchez, Adv. Funct. Mater. 14 (2004) 309–322.
[39] C.J. Brinker, Y. Lu, A. Sellinger, H. Fan, Adv. Mater. 11 (1999) 579–585.
[40] K. Wang, H. Wang, Y.-B. Cheng, Chem. Commun. 46 (2010) 303–305.
[41] P. Alexandris, J.F. Holzwarth, T.A. Hatton, Macromolecules 27 (1994) 2414–2425.
[42] Y. Ding, Y. Wang, R. Guo, J. Dispersion Sci. Technol. 24 (2003) 673–681.
[43] S.Y. Park, Y. Lee, K.H. Bae, C.-H. Ahn, T.G. Park, Macromol. Rapid Commun. 28 (2007) 1172–1176.
[44] J.M. Suh, S.J. Bae, B. Jeong, Adv. Mater. 17 (2005) 118–120.
[45] G.J.A.A. Soler-Illia, E. Scolan, A. Louis, P.A. Albouy, C. Sanchez, New J. Chem. 25 (2001) 156–165.
[46] G.J.A.A. Soler-Illia, A. Louis, C. Sanchez, Chem. Mater. 14 (2002) 750–759.
[47] A. Sundblom, A.E.C. Palmqvist, K. Holmberg, Langmuir 26 (2010) 1983–1990.